

Experimental analysis of hydrotreated vegetable oil (HVO) and commercial diesel fuel blend characteristics using modified CFR engine

M. Gailis^{1,2,*}, J. Rudzitis¹, J. Kreicbergs¹ and G. Zalcmanis¹

¹Riga Technical University, Faculty of Mechanical Engineering, Transport and Aeronautics, Department of Automotive Engineering, Viskalu 36A, LV 1006 Riga, Latvia

²Latvia University of Agriculture, Faculty of Engineering, Department of Mechanics, Liela street 2, LV 3001, Jelgava, Latvia

*Correspondence: maris.gailis@rtu.lv

Abstract. Performance parameters of different commercial diesel fuels is a subject of interest for fuel consumers. Fuel retailer Neste recently introduced a new brand of WWFC 5th grade diesel fuel in Baltic market, consisting of diesel fuel and hydrotreated vegetable oil (HVO) blend. Fuel samples have been recently tested on chassis dynamometer, measuring wheel power and torque and in road conditions, measuring fuel consumption. Evaluation of fuel consumption and performance parameters in road or laboratory conditions may yield uncertain results due to complexity of modern automobile engine management and emission reduction systems. To better evaluate the combustion, fuel samples have been tested in modified CFR engine at various intake air pressure, temperature and compression ratio settings. Engine indicated performance parameters and combustion phasing of regular diesel fuel and diesel fuel-HVO blend are presented. Comparing to regular diesel fuel, fuel blend with HVO showed reduced apparent heat release rate (AHRR) during premixed combustion phase at low inlet air temperature and low compression ratio conditions, comparing to regular diesel fuel. Premixed combustion phase AHRR of diesel-HVO blend increased above AHRR of regular diesel fuel at higher inlet air temperature and higher compression ratio conditions. Diffusion controlled combustion phase AHRR of diesel-HVO blend increased above AHRR of regular diesel fuel at higher inlet air temperature, higher compression ratio conditions and supercharged air supply.

Key words: Compression ignition, internal combustion, autoignition, heat release, ignition delay, IMEP, paraffinic fuel, NextBTL, biofuel, renewable fuel.

INTRODUCTION

Diesel fuels from renewable resources have been available in retail for some time. Traditionally those fuels are produced by esterification of vegetable oil and are not considered as premium fuel due to relative batch to batch variation of properties, low heating value, high cold filter plugging point, aging, water attraction, risk of biological contamination and high viscosity. Use of the first-generation biofuel, designated as 'Fatty Acid Methyl Ester' (FAME), is currently limited up to 7% volumetric blend in

EN590 summer grade diesel fuel. Use of neat FAME fuel is usually limited to pre-common rail era diesel powered automobiles. FAME is not added to winter grade diesel fuel in Nordic and Baltic countries. Another type of renewable diesel fuel has been recently commercialized. It is produced by hydrotreating vegetable or animal oils, and known as hydrotreated vegetable oil (HVO). Another designation for this product, used by oil producer Neste Group, is NextBTL. This promising renewable product contains mainly straight and branched alkanes, also known as paraffins. Other types paraffinic diesel fuel are gas to liquid (GTL) and Fischer-Tropsch (F-T) fuels. Paraffinic fuels does not contain oxygen and aromatics (Sajjad et al. (2014); Neste Group, 2016). As explained by Neste Group (2016), adding tens of percent HVO will improve lower grade base fuel properties and bring them up to the required standard. Premium grade diesel fuel, designated as 'Pro Diesel', has been introduced in Baltic market in 2016 by Neste Oil. This fuel is a blend of fossil diesel fuel and up to 15% vol. HVO. The interest of consumers on this product is high and fact based answers could be helpful. Effects of HVO and its blends with fossil diesel fuel on engine combustion, performance and emissions are investigated by many researchers, but some aspects are still unclear. Key properties of neat HVO are presented in Table 1. Neat HVO properties differ from EN590 standard diesel fuel mainly by cetane number, kinematic viscosity and density. HVO have higher heating value on mass basis, but lower density leads to lower volumetric heating value, comparing to typical EN590 fuel. Due to the differences, use of neat HVO may require recalibration of engine control system.

Aatola et al. (2008) investigated effect of injection timing on fuel consumption and regulated emissions using neat HVO and its blend with regular diesel fuel in heavy duty diesel engine with common-rail fuel injection system. Use of HVO with standard engine settings reduced nitrogen oxide (NO_x) production and gravimetric specific fuel consumption (SFC). Volumetric specific fuel consumption was increased with increase of HVO content in the blend. When injection timing was optimised for HVO, even greater emission reduction was found.

Sondors et al. (2014) used neat HVO and regular diesel fuel in the tractor Claas Ares 557ATX, equipped with engine John Deere 4045 with Stanadyne rotary distribution pump with electronic injection timing control. Engine power and torque was tested at full load conditions. Engine power and torque was decreased by approximately 5% and specific volumetric fuel consumption was increased by approximately 4% in tested engine whole speed range.

Pexa et al. (2015) compared in-line 4-cylinder Zetor 1204 engine performance characteristics using neat rapeseed methyl ester (RME) and neat HVO fuels. The engine was equipped with mechanical in-line injection pump, start of injection was 12° before top dead centre (TDC). They reported decrease of maximal engine power by 6.4%, using HVO. Difference in power and torque increased at higher engine speed. They found slight decrease of SFC, when HVO was used.

Napolitano et al. (2015) tested EN590 diesel fuel and hydrocracked diesel fuel-HVO blends in a light duty four cylinder 2 l diesel engine, equipped with closed loop combustion control, based on cylinder pressure trace analysis. Main injection timing was automatically adjusted to keep 50% mass fraction burning angle and indicated mean effective pressure (IMEP) close to target values, to cancel out differences of test fuel

properties. They assessed fuel consumption and exhaust emissions at steady state conditions, using various engine load and speed points within New European Driving Cycle (NEDC) range. It was found that combustion process differences between tested fuels decreased with higher engine load. Increase of HVO in fuel blend increased combustion stability, decreased volumetric fuel consumption and brake specific fuel consumption. Pellegrini et al. (2015) tested apparently similar samples of fuel as Napolitano et al. (2015), using single cylinder engine with variable compression ratio. Injection timing was corrected to achieve the same crank angle of 50% of fuel mass burned depending on test fuel. They reported reduction of unburned hydrocarbons and CO emissions with increase of HVO part in fuel. At high exhaust gas recirculation (EGR) rate, 30%, effect of added HVO on reduction of NO_x emissions was negligible. Test fuels had higher cetane number that was outside of the usual range of commercial diesel fuel. Pellegrini et al. (2015) and Napolitano et al. (2015) suggested that increase of cetane number by adding HVO in fuel was main contributor to combustion and emission differences between test fuels. Pellegrini et al. (2015) admitted that the methodology they used did not permitted to carry out a complete assessment of the fuels at constant engine setting parameters.

Karavalakis et al. (2016) assessed exhaust emissions and fuel economy from two heavy duty engines, Cummins ISX15 and ISB6.7. Both engines were equipped with current generation emission reduction systems. Testing was performed over the heavy-duty urban dynamometer driving schedule and heavy-duty diesel truck transient cycle, using CARB ULSD diesel fuel and diesel-HVO blends. Fuel economy, calculated using carbon balance method, was reduced in case of Cummins ISB6.7 with increase of HVO fraction in blend, but not in case of ISB6.7 engine.

Most researchers reported that use of HVO in diesel fuel blend reduced unburned hydrocarbon and CO emissions. Effect of adding HVO in diesel fuel blend on emissions of NO_x and particle matter, fuel consumption and engine torque and power is less clear and appears to be dependent on test conditions. Effect of HVO and other paraffinic fuel in diesel fuel on combustion phasing in some research reports is masked by corrected injection timing (Napolitano et al. 2015, Pellegrini et al. 2015). This approach is very useful to reveal possible benefits of paraffinic diesel fuel in future applications, where engine control system can adapt to fuels with different autoignition properties. Majority of actual practical diesel engine control systems do not have control loop with combustion process feedback. Sugiyama et al. (2011) reported that injection quantity using HVO is increased, comparing to diesel fuel. Using different injection timing and injected fuel volume for each test fuel and cetane number that is out of regular range, difference in combustion properties of diesel fuel un diesel – HVO blend is unclear.

This study differs from the work of other researchers by using standard engine type – CFR, and commercial grade diesel fuel – HVO blend with cetane number adjusted within standard range. By setting constant injection timing and injected fuel volumetric amount for standard diesel fuel and diesel fuel – HVO blend, and no pilot injection, autoignition and combustion properties of test fuels are clearly shown in various compression ratios, inlet air pressure un temperature.

MATERIALS AND METHODS

Experimental work was conducted at Riga Technical University, Engine Laboratory of Department of Automotive Engineering, January 2017.

Test Fuels

The fuels used in this study were purchased at the same time and the same Neste Latvia retail station on May 2016. Regular diesel fuel was designated as ‘Artic Fuel, Class 0’ and did not contain FAME. Properties of test fuels were obtained from refinery certificate of quality and are presented in Table 1. Only regular diesel fuel (D) and HVO-diesel fuel blend (DHVO) were used in testing. Properties of neat HVO are included for comparison. Fuels were stored in clean polyethylene containers.

Table 1. Properties of test fuel and neat HVO

Fuel	D	DHVO	HVO*
Density at 15 °C, kg m ⁻³	824.4	822.2	775...785
Cetane number	51.1	55.0	80...99
Cetane index	47.9	52.0	> 56.5
Viscosity at 40 °C, mm ² s ⁻¹	1.937	2.537	3.500
Polyaromatics. % vol.	1.3	1.1	0.0
FAME. % vol.	0.0	0.0	0.0
HVO. % vol.	0.00	9.15	100.00

*HVO properties according to Aatola et al. (2008)

HVO consists of different alkanes (paraffins). It is known that addition of normal alkanes with long chain length to diesel fuel shortens autoignition time and increases cetane number (Glavincevski et al., 1984). Cetane index was introduced due to complexity and expenses of experimental determination of cetane number. Cetane index was not intended to use for alternative fuels, such as HVO (Murphy 1983; Bezaire et al., 2010). That explains high cetane number and approximate cetane index for neat HVO, shown in Table 1.

Engine and Instrumentation

The experimental setup consisted of single cylinder four stroke compression ignition engine, coupled with asynchronous electric motor, critical flow nozzle air flow meter, inlet air heater and in-cylinder pressure indicating system. The test engine technical characteristics are close to CFR F5 engine, which is a standard equipment for cetane number determination. The engine features 2-valve cylinder head with cylindrical variable volume pre-chamber. Engine compression ratio (CR) can be continuously changed by moving the plug in the pre-chamber. In-line high pressure fuel pump has micrometer type controls for setting fuel delivery rate and injection timing. Fuel is injected in the pre-chamber and the injector is equipped with a needle position switch.

Asynchronous electric motor maintains constant rotational frequency for motoring and firing. Critical flow nozzle is used for controlling inlet air mass flow and pressure, allowing imitation of naturally aspirated and supercharged engine operation. Engine air supply system is equipped with an inlet air heater and a surge tank. Main characteristics of the test engine are presented in Table 2.

Table 2. Characteristics of the test engine

Parameter	Value
Engine type	IDT69
Air supply	Controlled pressure and temperature
Coolant temperature, °C	100 ± 2
Bore and stroke, mm	85 × 115
Cylinder volume, cm ³	652
Compression ratio	7 : 1 to 23 : 1
Fuel injector opening pressure, MPa	10.4 ± 0.4
Diameter of cylindrical pre-chamber, mm	42
Inlet valve opens/ closes, deg	10° ± 2° ATDC / 34° ± 2° ABDC
Exhaust valve opens/ closes, deg	40° ± 2° BBDC / 15° ± 2° ATDC
Valve overlap, deg	5° ± 2°
Engine speed, min ⁻¹	900 ± 10
Power of absorbing electric motor, kW	5.5

In-cylinder pressure is measured in pre-chamber, using pressure transducer Kistler 6061B and charge amplifier Kistler 5018A. Inlet air pressure is measured using pressure transducer Omega MMA100. Inlet air temperature is measured with K-type thermocouples. Crankshaft angular position is detected using encoder EPC 702, with the resolution 0.1 crank angle degree (CAD). Data acquisition system is based on National Instruments chassis NI9068 and various input modules. In-house LabVIEW code was developed, allowing monitoring and data saving during the tests. More detailed description of this test engine setup can be found in Gailis et al. (2016).

Test Methodology

Test engine was started and warmed up to stabilise oil temperature around 40 °C and coolant temperature at 100 ± 2 °C. Engine speed was held constant at 900 ± 10 min⁻¹. Before each test the start of injection (SOI) was set at 13° before top dead centre (BTDC) and fuel delivery rate was set at 13 ml min⁻¹. These settings were based on typical conditions for cetane number determination, using CFR engine. SOI was influenced by CR and inlet air pressure. Rising CR from 14 to 16 increased SOI advance by 1.5 CAD. Rising inlet air pressure by 0.7 bar increased SOI advance by approximately 2 CAD. SOI was adjusted before the test and monitored during the test. Design of the injector and low injection pressure were presumable reasons for this phenomenon.

Engine stabilization time between tests was 180 s in case of compression ratio or inlet air pressure change and 1,200 s in case of fuel change. Variable testing parameters are listed in Table 3. Testing was conducted in eight steady state operation points for both fuels. All combinations of parameter setup were tested. During each test data of 150 consecutive engine cycles were collected. To statistically evaluate the results, each test was non-consecutively repeated three times.

Table 3. Test conditions

Parameter	Value
Test fuel I	D
Test fuel II	DHVO
Inlet air temperature I, °C	65
Inlet air temperature II, °C	95
Compression ratio I	14 : 1
Compression ratio II	16 : 1
Inlet air pressure I, bar	1.0
Inlet air pressure II, bar	1.7

Data Processing

Data post processing and report generation is performed using in-house developed MATLAB code. Mean value of 150 consecutive engine cycles is used for cylinder pressure data analysis. Apparent heat release rate (AHRR) is calculated using Eq. (1) according to Stone (1999).

$$\frac{dQ_n}{d\varphi} = \frac{\gamma}{\gamma - 1} p \frac{dV}{d\varphi} + \frac{\gamma}{\gamma - 1} V \frac{dp}{d\varphi} \quad (1)$$

where dQ_n – apparent heat release rate, J deg⁻¹; φ – crank angle degree; γ – ratio of specific heats; V – cylinder volume, m³; p – cylinder pressure, Pa.

Polytropic exponent is used as ratio of specific heats and calculated by finding polynomial fit coefficient for cylinder pressure and volume relation in logarithmic scale. Polytropic exponent is calculated separately for compression and expansion stroke of each engine cycle and mean value is used as ratio of specific heats for AHRR calculation. Value of polytropic exponent was different for each engine cycle. Approximate value of polytropic exponent was 1.3.

Cumulative heat release (CHR) is calculated using Eq. (2) according to Heywood (1988).

$$Q_n = \int_{\varphi_{start}}^{\varphi_{end}} \frac{dQ_n}{d\varphi} d\varphi \quad (2)$$

where Q_n – cumulative heat release rate, J.

Relative cumulative heat release (RCHR) is calculated from CHR and stated in percent. RCHR is used for combustion phasing analysis. Duration of RCHR from start of combustion (SOC) to 30% is designated as initial combustion phase. Premixed combustion dominates in this phase. Duration of RCHR from 30% to 75% is designated as early combustion phase. Diffusion controlled combustion dominates in this phase. Duration of RCHR from 75% to 90% is designated as late combustion phase.

Indicated work is calculated using Eq. (3) according to Heywood (1988).

$$W_i = \int_{\varphi_{start}}^{\varphi_{end}} p dV \quad (3)$$

where W_i – indicated work, J.

Gross indicated work is calculated only in compression and expansion strokes, so gas exchange work is excluded from the result. Indicated mean effective pressure (*IMEP*) is calculated from gross indicated work, using Eq. (4) according to Heywood (1988).

$$IMEP = \frac{W_i}{V_d} \quad (4)$$

where *IMEP* – indicated mean effective pressure, bar; V_d – displaced cylinder volume, m³.

To compare work efficiency of engine cycle between test conditions and fuels, IMEP is also calculated from indicated work, which is calculated in smaller intervals of 5 CAD. Difference between data points of the two tests of interest is calculated and analysed.

Temperature of charge at start of injection (SOI) is calculated using ideal gas law and Eq. (5).

$$T_{SOI} = \frac{p_{SOI} \cdot V_{SOI}}{m \cdot R_i} \quad (5)$$

where T_{SOI} – temperature at SOI, K; V_{SOI} – volume at SOI, m³; m – mass of charge, kg; R_i – specific gas constant of air, J kg⁻¹ K⁻¹.

Mass of charge is calculated using ideal gas law, taking inlet air temperature, in-cylinder pressure and volume after inlet valve closure.

RESULTS AND DISCUSSION

The results presented in this sub-chapter are arranged by compression ratio and inlet charge pressure.

Heat Release Rate Analysis

Cylinder pressure trace, averaged from 150 consecutive engine cycles is shown in Fig. 1, a & 1, b. Injector needle position switch signal indicated that injection time was constant for both fuels at all tested conditions. Duration of injection was 17 CAD and end of injection was 4° after top dead centre (ATDC).

AHRR trace is basically output of a simple thermodynamic model, which describes how much heat would have to be added, to produce observed pressure variations, assuming adiabatic compression and expansion process due to cylinder volume change (Stone 1999). The results of AHRR and RCHR calculation in conditions CR14/P1.0/T65 are shown in Fig. 1, c.

The ignition delay is followed by premixed combustion period. In this period, rapid combustion of evaporated fuel, which is mixed with the air within flammability limits occurs. In case, shown in Fig. 1, c, calculated bulk charge temperature at SOI is 627 K and measured cylinder pressure is 25.4 bar. Premixed combustion phase lasts from approximately 7° BTDC till 8° ATDC for both fuels. Heat release during premixed combustion phase rate is significantly higher for fuel D. Ignition delay difference for both test fuels is very small. Comparingly smaller amount of evaporated, mixed and burned fuel can be assumed in case of fuel DHVO. This can be attributed to different evaporation properties of HVO, comparing to diesel fuel. Distillation curves are presented in works of Aatola et al. (2011) and Napolitano et al. (2015). Approximately 50% of energy is released during premixed stage of combustion, using regular diesel fuel, comparing to 42% for DHVO fuel. Diffusion controlled combustion phase and late combustion phase appears to be extended for fuel DHVO, comparing to fuel D.

The results of AHRR and RCHR in conditions CR14/P1.0/T95 are shown in Fig. 1, d. Calculated charge temperature at SOI is 659 K and measured cylinder pressure is 24.7 bar. Due to relatively large ignition difference delay between fuels, premixed combustion of fuel DHVO starts at lower temperature and pressure, comparing to fuel D. Diffusion controlled combustion phase and late combustion phase appears to be extended for fuel DHVO, comparing to fuel D.

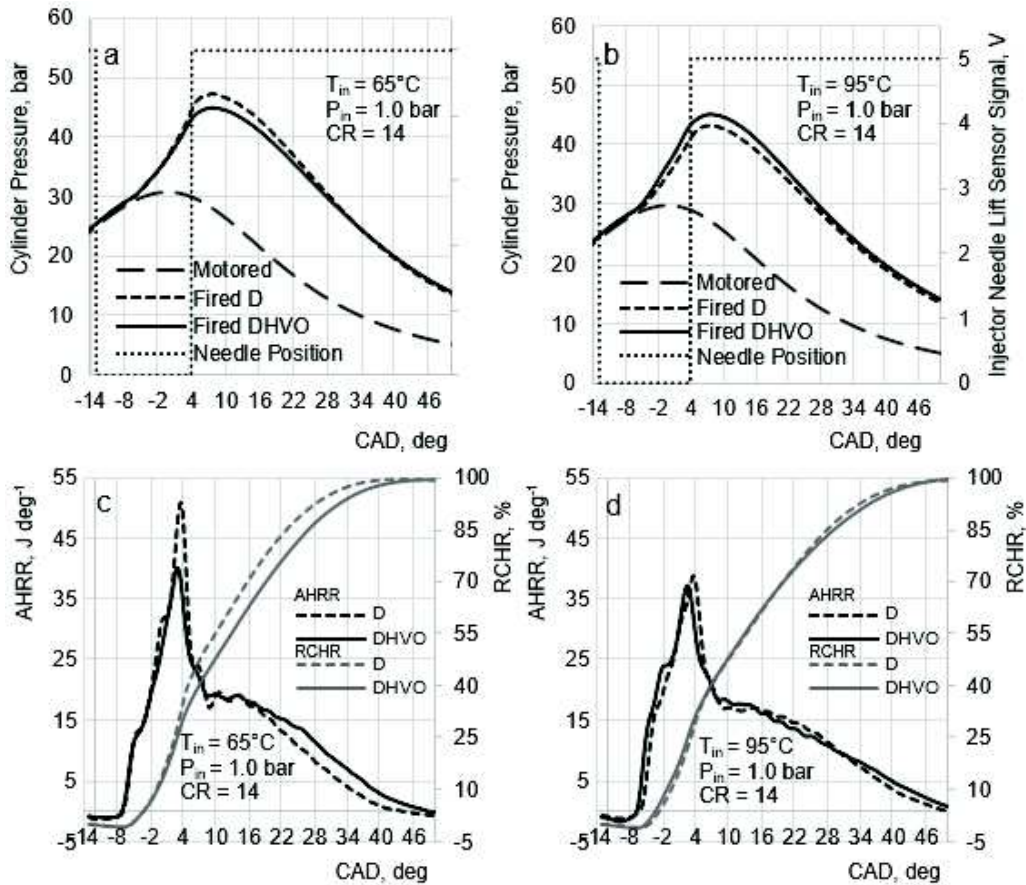


Figure 1. Cylinder pressure trace and injector needle position switch signal trace, apparent heat release rate and relative cumulative heat release, naturally aspirated mode, compression ratio 14 : 1.

The results of AHRR and RCHR in conditions CR14/P1.7/T65 are shown in Fig. 2, c. Supercharged operating mode is imitated in this case. Calculated charge temperature at SOI is 603 K and measured cylinder pressure is 43.3 bar. Premixed combustion phase is extended for fuel DHVO, comparing to fuel D. During diffusion controlled combustion phase, which lasts approximately from 7° to 24° ATDC, fuel D have higher AHRR and this phase is shorter for fuel D. The difference in diffusion phase duration is also shown in Fig. 8, a. During late combustion stage, fuel DHVO shows apparently higher AHRR.

The results of AHRR and RCHR in conditions CR14/P1.7/T95 are shown in Fig. 2, d. Calculated charge temperature at SOI is 649 K and measured cylinder pressure is 42.3 bar. Increase of initial charge temperature shortens premixed combustion phase for fuel DHVO, while having little effect on fuel D. AHRR during early diffusion controlled combustion phase is higher for fuel DHVO.

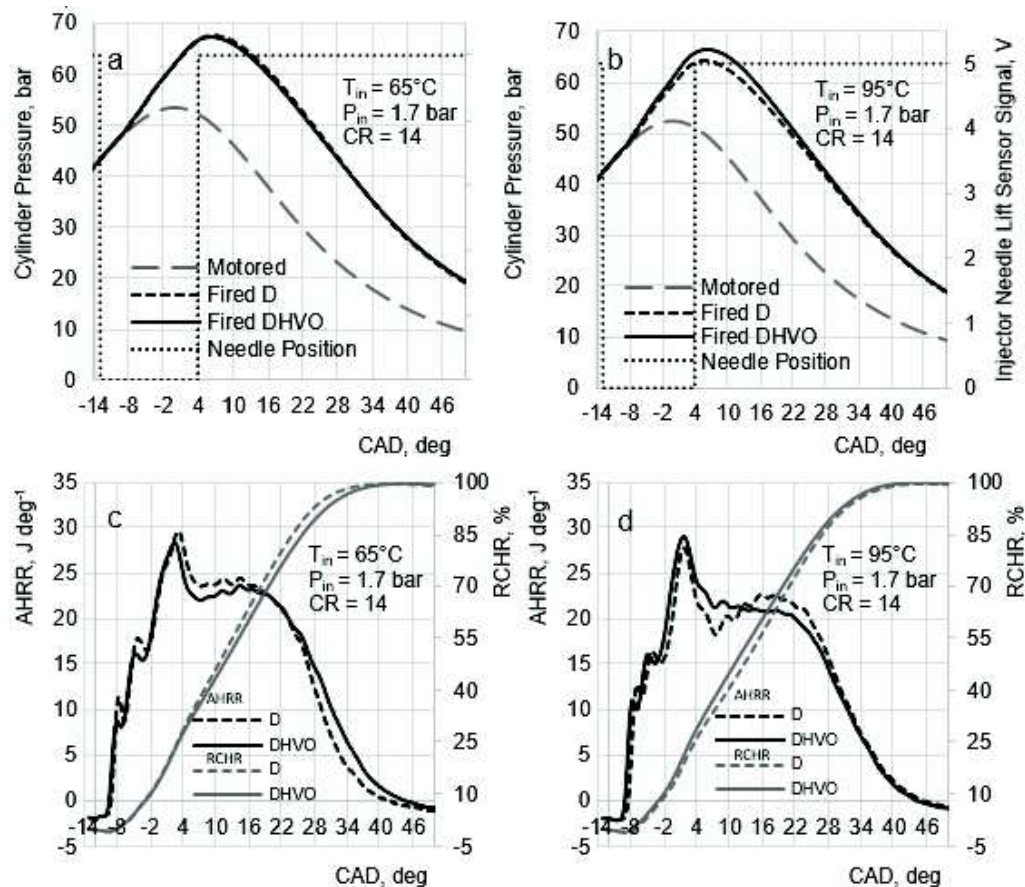


Figure 2. Cylinder pressure trace and injector needle position switch signal trace, apparent heat release rate and relative cumulative heat release, supercharged mode, compression ratio 14 : 1.

The results of AHRR and RCHR in conditions CR16/P1.0/T65 are shown in Fig. 3, c. Calculated charge temperature at SOI is 634 K and measured cylinder pressure is 29.1 bar. Difference in ignition delay between the both fuels is quite large. Despite of shorter ignition delay, premixed combustion of fuel DHVO starts and continues with higher AHRR, comparing to fuel D. During diffusion controlled combustion phase AHRR for fuel DHVO is significantly lower. Apparently, in this case, conditions for diffusion are more beneficial for fuel D.

The results of AHRR and RCHR in conditions CR16/P1.0/T95 are shown in Fig. 3, d. Ignition delay difference between test fuels is smaller, but combustion phasing is like in previous case.

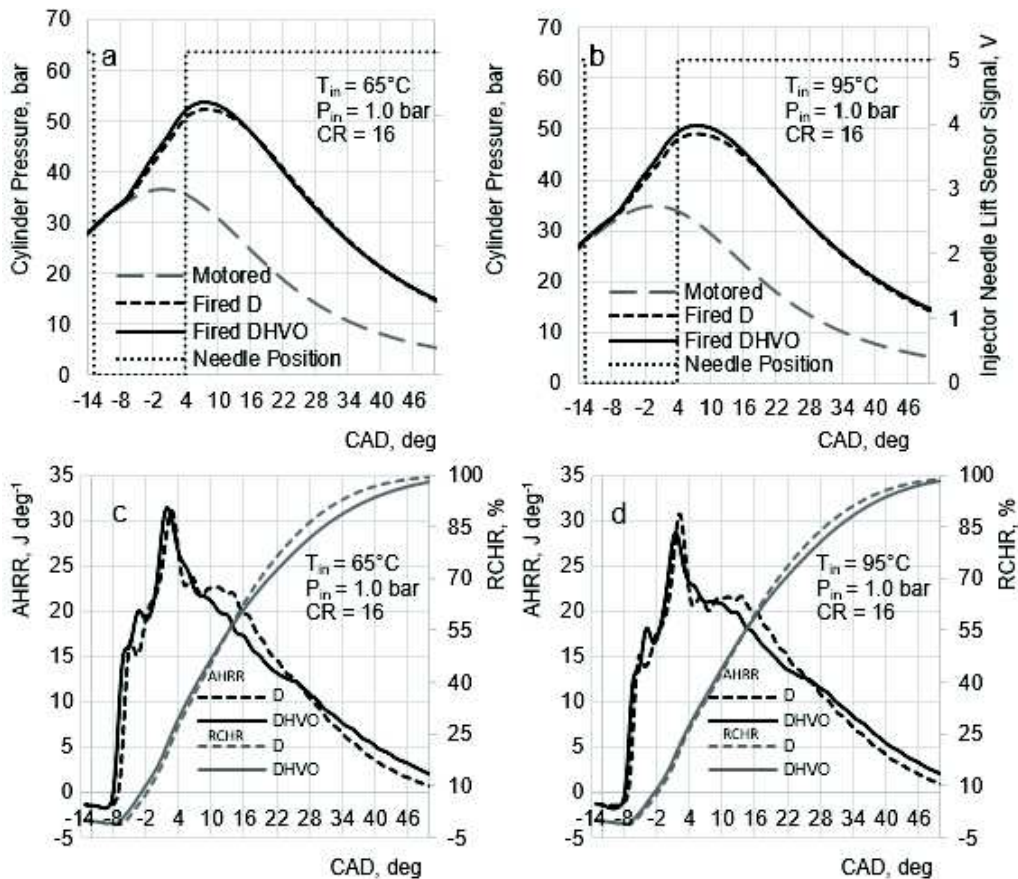


Figure 3. Cylinder pressure trace and injector needle position switch signal trace, apparent heat release rate and relative cumulative heat release, naturally aspirated mode, compression ratio 16 : 1.

The results of AHRR and RCHR in conditions CR16/P1.7/T65 are shown in Fig. 4, c. Calculated charge temperature at SOI is 614 K and measured cylinder pressure is 49.2 bar. Ignition delay is very close to the values of the case of CR14/P1.7/T65. By comparing those cases, it can be noticed that behaviour of the test fuels during premixed combustion phase is different. In this case, where initial charge temperature is higher, AHRR during early premixed combustion stage is higher for fuel DHVO, comparing to fuel D. The trend is opposite in lower charge temperature. During diffusion controlled combustion phase AHRR is lower for fuel DHVO and this phase is insignificantly extended, comparing to fuel D.

The results of AHRR and RCHR in conditions CR16/P1.7/T95 are shown in Fig. 4, d. Calculated charge temperature at SOI is 671 K and measured cylinder pressure is 48.3 bar. Absolute value of the ignition delay is very small and such is the absolute

difference in ignition delay between test fuels. AHRR trace is similar for both fuels during premixed combustion stage. Low value of AHRR during this stage can be explained by raised temperature and pressure, comparing to another test modes.

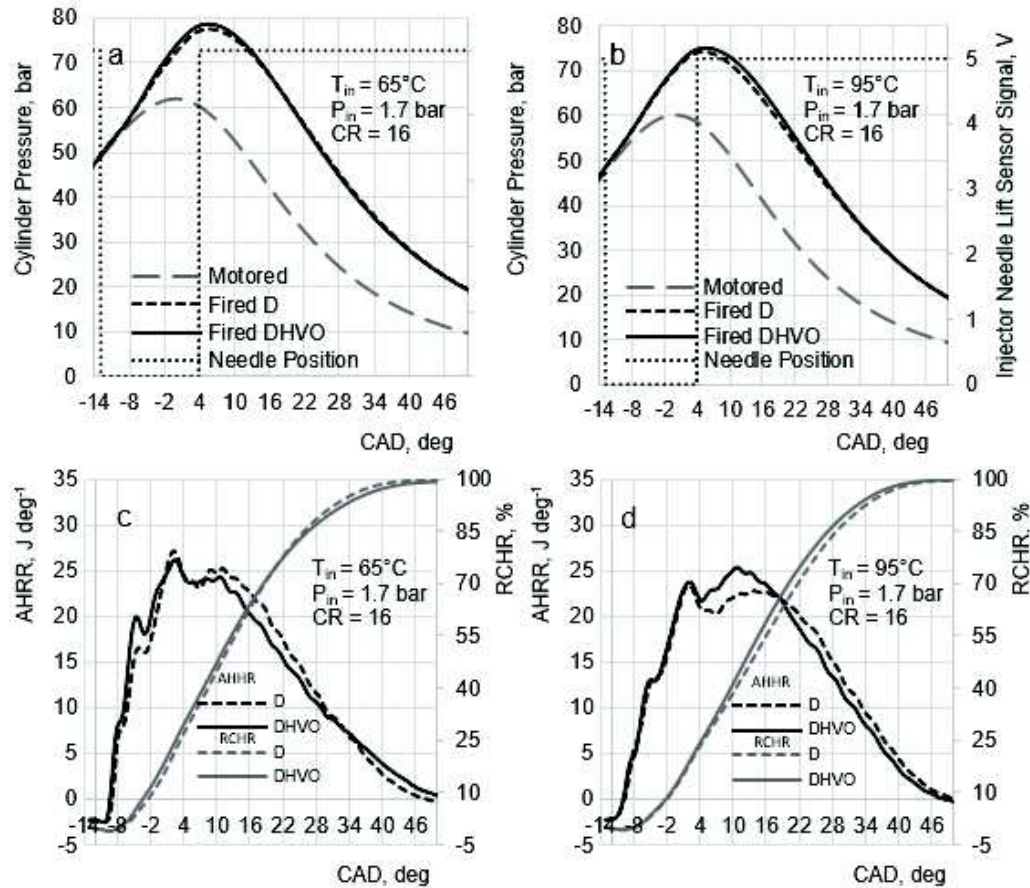


Figure 4. Cylinder pressure trace and injector needle position switch signal trace, apparent heat release rate and relative cumulative heat release, supercharged mode, compression ratio 16 : 1.

During diffusion controlled combustion AHRR is higher for fuel DHVO. At very late combustion stage AHRR is lower for fuel DHVO. This trend is opposite in another tested conditions.

Ignition Delay

Evaporation of the injected fuel decreases charge temperature and AHRR becomes negative following injection. Ignition delay is assumed as duration in engine cycle between SOI and the moment when AHRR becomes positive due to chemical energy release. During the ignition delay fuel droplets are evaporated and mixed with the air. The ignition delay is affected by physical factors such as pressure, temperature and charge motion and properties of the fuel. In this experiment, physical factors at the SOI point were kept similar for both test fuels. According to Heywood (1988), physical

characteristics of the regular diesel fuel, such as vaporization rate and viscosity, does not significantly affect ignition delay in partially or fully warmed engines. Chemical properties of the fuel are another major contributor to ignition delay. A widely-used measure ability of the fuel to autoignite is cetane number. Cetane number was higher for test fuel DHVO, so shorter ignition delay for this fuel was expected.

Shorter ignition delay results in lesser amount of injected fuel mass before the combustion begins. Conditions, such as pressure and temperature, are constantly changing in the combustion chamber of the reciprocating engine during engine cycle due to movement of the piston. In this study SOI is kept constant between different tests.

If conditions for both test fuels are similar at SOI, differences in ignition delay will result in different conditions at start of combustion.

Ignition delay is shown in Fig. 5. Absolute values were mostly affected by inlet air pressure. Shortest ignition delays are found during supercharged test conditions. Error bars in all following diagrams represent confidence interval, calculated with the significance $P = 0.05$. Statistically significant result of ignition delay difference between tested fuels is obtained only in CR14/P1.7/T65 test conditions.

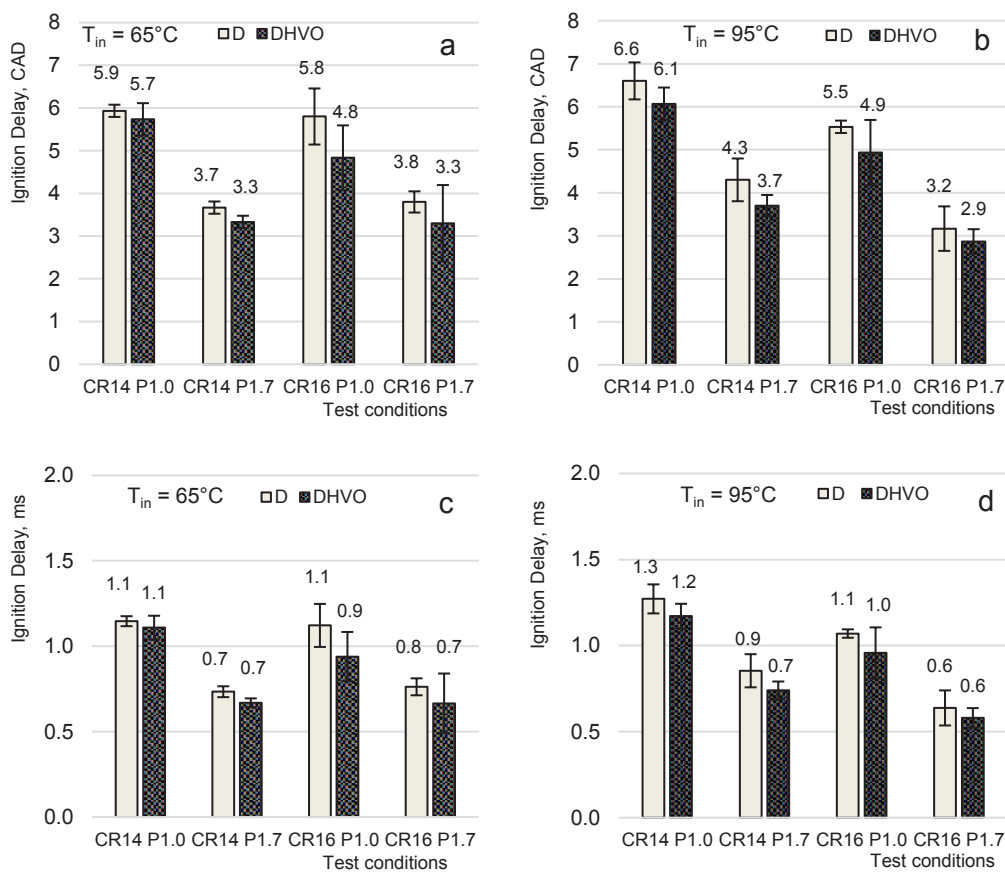


Figure 5. Ignition delay in all test modes.

Differences between ignition delay of test fuels are shown in Fig. 6. Ignition delay is shorter for fuel DHVO in all tested conditions. Difference is ignition delay between test fuels is less dependent from changes of CR and inlet charge pressure at higher initial charge temperature.

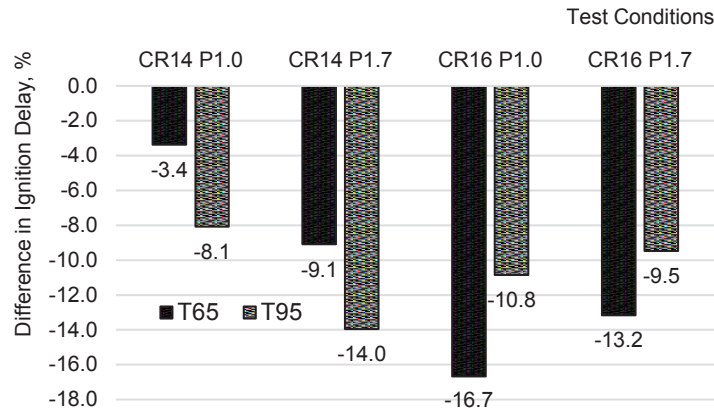


Figure 6. Difference in ignition delay in all test modes.

Shorter ignition delay for fuel DHVO leads to lower temperature and pressure at the start of combustion. It can be assumed, that in case of fuel DHVO, less fuel is evaporated and mixed with air during ignition delay.

Combustion Phasing

Duration of initial combustion phase is shown in Fig. 7. Mainly premixed combustion is dominating in this phase. Results are statistically insignificant, but fuel DHVO shows a trend of longer initial combustion phase in test conditions of low charge temperature and low charge pressure. In this analysis, lower AHRR can be assumed, if analysed phase is extended.

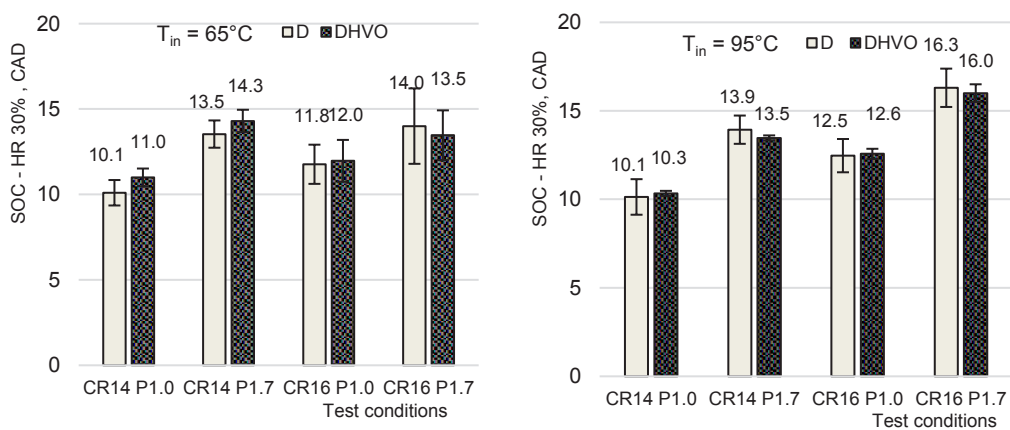


Figure 7. Duration of initial combustion phase, from start of combustion to 30% of relative cumulative heat release.

Duration of early combustion phase is shown in Fig. 8. Mainly diffusion controlled combustion is present in this phase. Results are mostly statistically insignificant, but fuel DHVO shows a trend of longer diffusion controlled combustion phase in tested conditions, where charge temperature and pressure are lower. At test conditions, where charge temperature was high and pressure highest, early combustion phase for fuel DHVO was shorter than for fuel D.

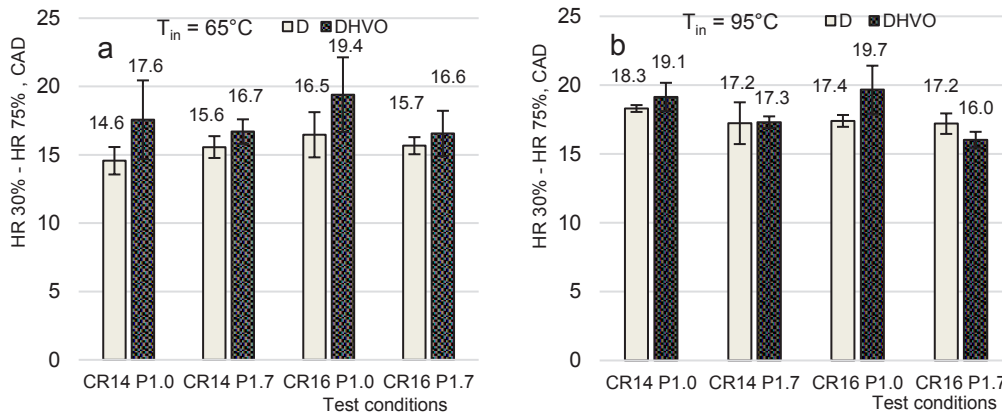


Figure 8. Duration of early combustion phase, from 30% to 75% of relative cumulative heat release.

Duration of late combustion phase is shown in Fig. 9. Fuel DHVO shows a trend of longer late combustion phase in all tested conditions. Difference between length of late phase of combustion for compared fuels is statistically insignificant but appears to diminish with higher charge temperature and pressure.

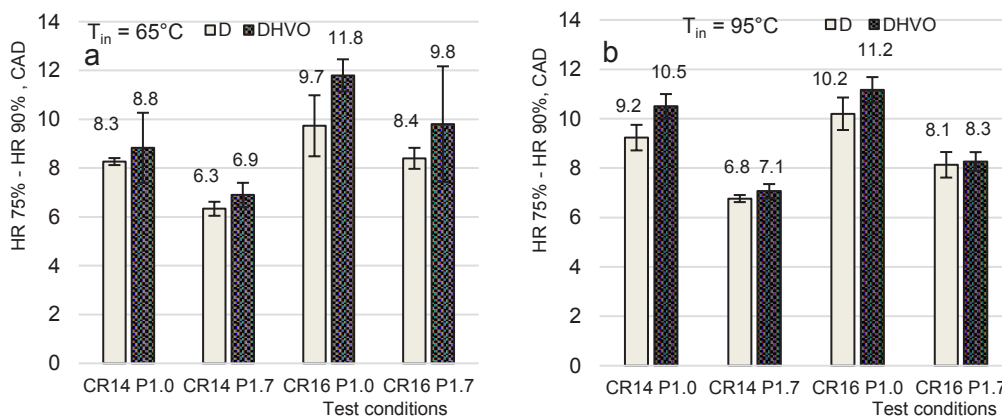


Figure 9. Duration of late combustion phase, from 75% to 90% of relative cumulative heat release.

Duration of combustion is shown in Fig. 10. Fuel DHVO shows trend of longer duration of combustion in conditions when inlet air temperature is 65 °C, comparing to fuel D. Raised inlet air temperature at 95 °C appears to have larger effect on combustion duration of fuel D.

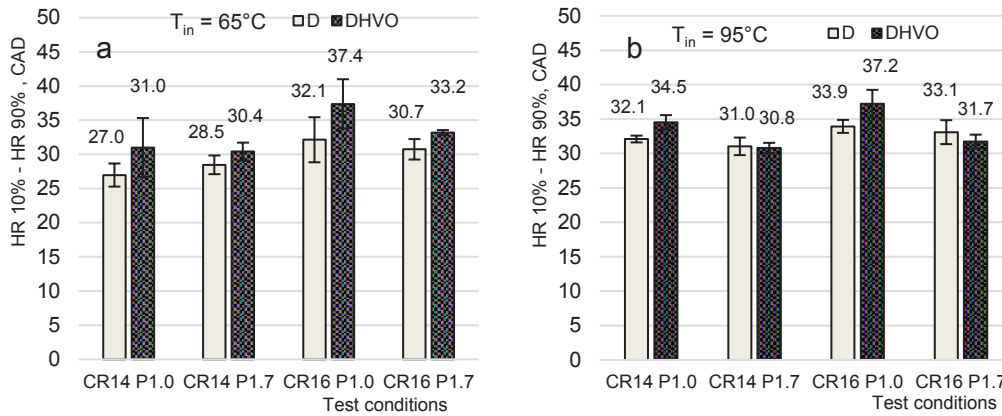


Figure 10. Duration of combustion, from 10% to 90% of relative cumulative heat release.

Phasing of combustion at 50% of released heat is shown in Fig. 11. Phasing is shown in crank angle degrees after TDC. Phasing is later in engine cycle at low compression ratio (CR14) and low inlet charge temperature for fuel DHVO, comparing to fuel D. This can be attributed to extended premixed and diffusion controlled combustion phases for fuel DHVO at low temperature and pressure conditions.

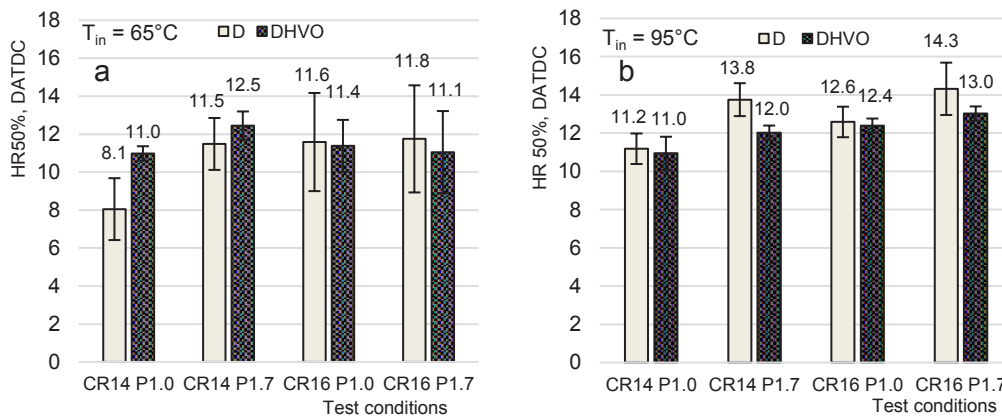


Figure 11. Phasing of combustion, CAD after TDC for 50% of relative cumulative heat release.

Assumed phasing of the end of combustion at 90% of released heat is shown in Fig. 12. End of combustion appears to be phased later in engine cycle for fuel DHVO at low temperature and low pressure conditions. At test conditions, where charge temperature and pressure is relatively high, end of combustion for fuel DHVO is earlier

in engine cycle than for fuel D. Difference between ends of combustion for compared fuels is statistically insignificant at tested conditions.

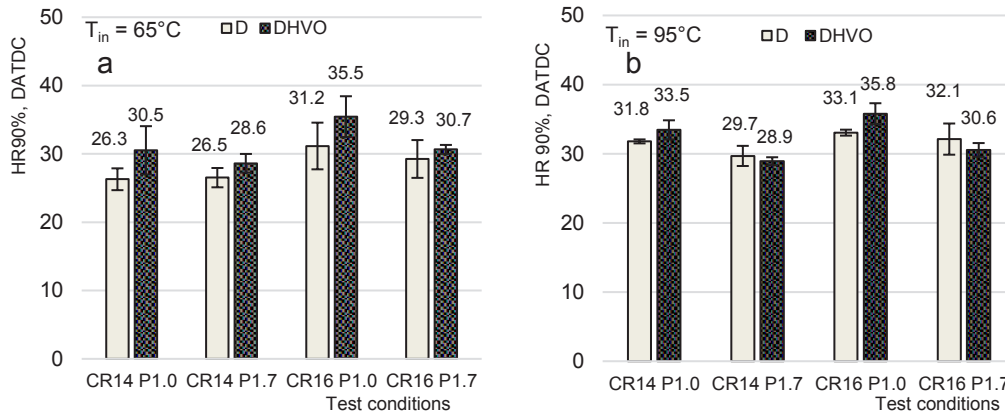


Figure 12. The end of combustion, CAD after TDC for 90% of relative cumulative heat release.

Comparison of gross IMEP between tested fuels is shown in Fig. 13. The volume of injected fuel and injection timing is held constant at all test modes. Heating values of neat HVO and EN590 grade diesel fuel were reported by Aatola et al. (2008). Volumetric heating value of fuel, containing HVO, is expected to be slightly lower, comparing to regular diesel fuel. Higher values of gross IMEP, when DHVO fuel is used, are found at all tested conditions, except CR16/P1.7/T95. Differences between fuels are larger when initial charge temperature is 95 °C. As pressure changes in the main combustion chamber is not included in calculation of IMEP, these results are not entirely reliable.

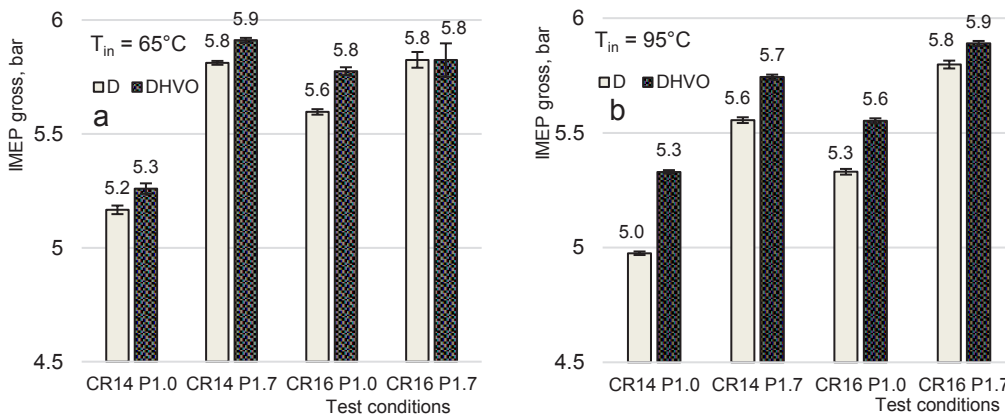


Figure 13. Gross indicated mean effective pressure (IMEP) at all test conditions.

Indicated Work Output

To analyse causes of IMEP variation between tests and tested fuels, IMEP is calculated in limited steps with length of 5 CAD for each averaged engine cycle. Difference between data points of both test fuels is calculated by subtraction the result

for fuel D from the result for fuel DHVO. CAD based difference of IMEP between tested fuels is shown in Fig. 14. Positive value means that work output of fuel DHVO is higher at given point. Results reveal difference of work output during engine cycle between tested fuels.

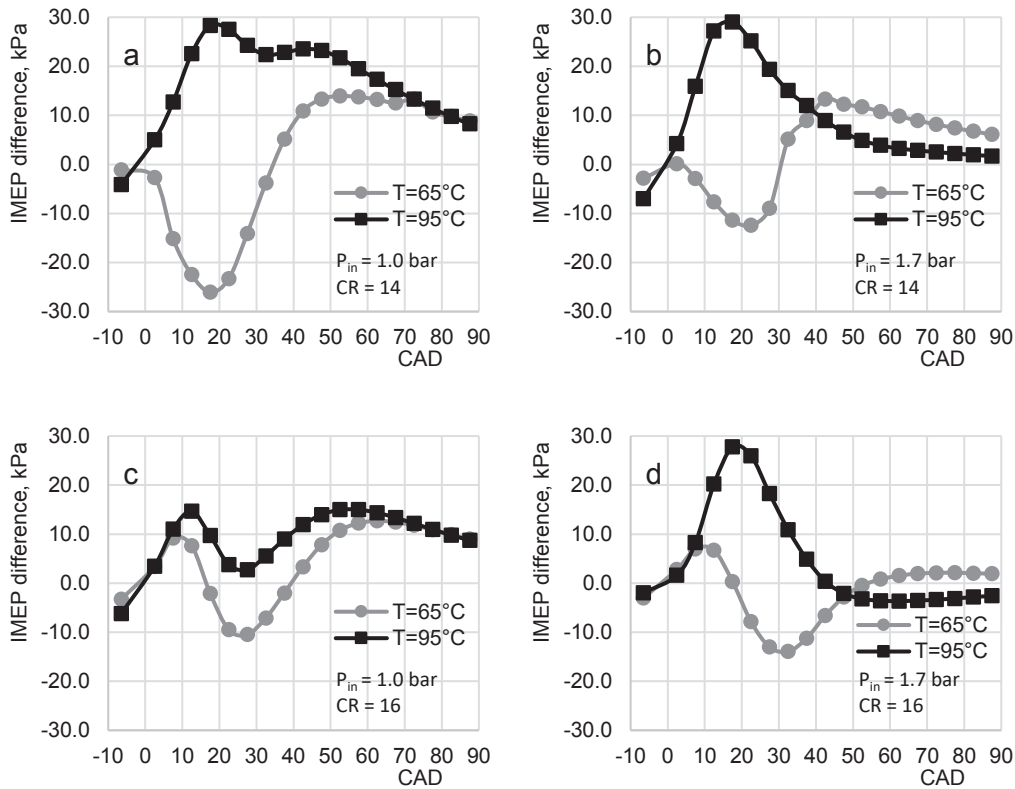


Figure 14. Difference between indicated work output during expansion stroke using fuels DHVO and D at all test conditions.

At low inlet air temperature (65°C) and low compression ratio (CR14), premixed combustion phase (Fig. 7, a) and diffusion controlled combustion phase (Fig. 8, a) is extended using DHVO fuel. Energy release is retarded in engine cycle in case of DHVO fuel. In first part of expansion stroke work output is higher for fuel D, which is shown in Figs 14, a & 14, b, lines $T65^\circ\text{C}$.

At the same inlet air temperature (65°C) but with increased compression ratio (CR16), premixed combustion phase (Fig. 7, a) is shorter for fuel DHVO and it reflects on work output difference between test fuels. Higher work output for fuel DHVO in the very beginning of expansion stroke is shown in Figs 14, c & 14, d, lines $T65^\circ\text{C}$.

At higher inlet air temperature (95°C) premixed combustion phase (Fig. 7, b) is shorter using DHVO fuel than using fuel D. In conditions of naturally aspirated air supply ($P_{in} 1.0$), diffusion controlled combustion phase (Fig. 8, b) for fuel DHVO is longer than for fuel D. Energy release is retarded in engine cycle in case of DHVO fuel. Work output is higher for fuel DHVO at the beginning of expansion stroke, following by lower

values during diffusion controlled combustion and increased again from 50 CAD which is shown in Figs 14, a & 14, c, lines T95 °C.

In conditions of supercharged air supply (P1.7), premixed combustion phase (Fig. 7, b) and diffusion controlled combustion phase (Fig. 8, b) is shorter for fuel DHVO comparing to fuel D. Work output is higher for fuel DHVO in the first part of expansion stroke, which is shown in Figs 14, c and 14, d, lines T95 °C.

Cyclic Variation

Stability of engine operation can be characterized by variation of IMEP between engine cycles. According to Heywood (1988), vehicle driveability is affected, when coefficient of variation of IMEP (COV IMEP) exceeds 10%. Calculated results of COV IMEP gross are shown in Fig. 15. Overall values of COV IMEP are sufficiently low. No trend for COV IMEP dependency on tested fuels is found at tested conditions.

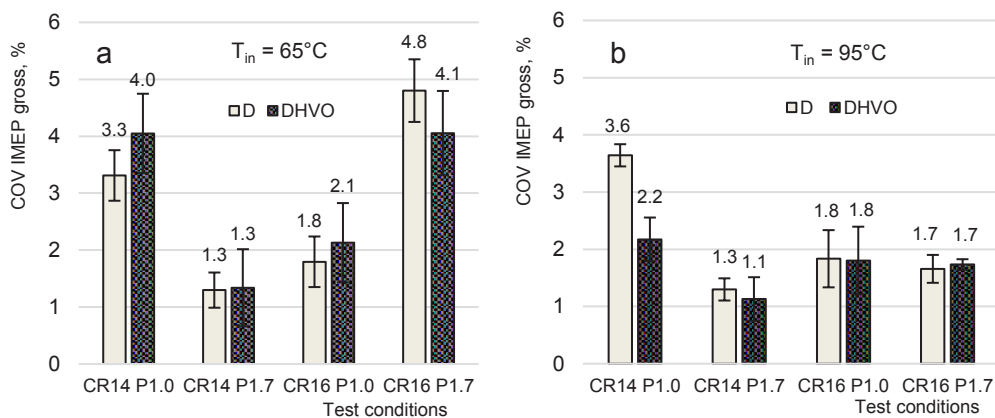


Figure 15. Covariation of gross IMEP at all test conditions.

CONCLUSION

The following conclusions from the results obtained in this study can be made:

- Ignition delay using DHVO fuel at inlet air temperature 95 °C is approximately 8...11% shorter than using fuel D.
- Absolute difference in ignition delay between test fuels diminishes with increase of inlet air temperature, pressure and compression ratio.
- Tested commercial fuels appear to have different combustion phasing, depending on test conditions.
- At inlet air temperature 65 °C, naturally aspirated air supply and compression ratio 14 : 1 AHRR of premixed combustion phase is reduced and duration extended for fuel DHVO, comparing to fuel D. The results are statistically insignificant.
- Increase of inlet air temperature at compression ratio 14 : 1 appears to increase AHRR and shorten duration of premixed combustion phase for fuel DHVO, while having little effect on fuel D.

- Increase of compression ratio at inlet air temperature 65 °C appears to increase AHRR and shorten duration of premixed combustion phase for fuel DHVO, comparing to fuel D. The results are statistically insignificant.
- At inlet air temperature 65 °C, compression ratio 14 : 1 and naturally aspirated air supply AHRR of diffusion controlled combustion phase is reduced and duration extended for fuel DHVO, comparing to fuel D. The results mostly are statistically insignificant.
- Late combustion phase appears to be extended for fuel DHVO in tested conditions, comparing to fuel D. The results are not statistically significant.
- 50% on released energy is achieved later in engine cycle at inlet air temperature 65 °C and compression ratio 14 : 1 for fuel DHVO, comparing to fuel D. The results are statistically insignificant.

This study reveals differences between tested commercial fuels in sensitivity and response of heat release rate during premixed and diffusion controlled combustion to variations in basic conditions, such as inlet air temperature, compression ratio and inlet air pressure. Impact of combustion differences on work output in engine cycle is shown. Depending on practical engine design and working conditions, those differences may influence performance parameters and exhaust gas composition.

ACKNOWLEDGEMENTS. Professor Marcis Jansons is thanked for providing advice and some essential parts of research hardware.

REFERENCES

- Aatola, H., Larmi, M., Sarjoavaara, T. & Mikkonen, S. 2008. Hydrotreated Vegetable Oil (HVO) as a Renewable Diesel Fuel: Trade-off between NO_x, Particulate Emission, and Fuel Consumption of a Heavy Duty Engine. SAE Technical Paper 2008-01-2500. *SAE Technical Papers* **724**, 12 p.
- Bezaire, N., Wadumesthrige, K., Simon Ng, K.Y. & Salley, S.O. 2010. Limitations of the use of cetane index for alternative compression ignition engine fuels. *Fuel* **89**(12), 3807–3813.
- Gailis, M., Jansons, M., Rudzitis, J. & Kreicbergs, J. 2016. Instrumentation of cetane number research engine. In: *Engineering for Rural Development*. Jelgava: LUA, Jelgava, pp. 1424–1429.
- Glavinčevski, B., Gülder, Ö. & Gardner, L. 1984. Cetane Number Estimation of Diesel Fuels from Carbon Type Structural Composition. *SAE Technical paper* **841341**, 12 p.
- Heywood, J.B. 1988. *Internal Combustion Engine Fundamentals*. McGraw-Hill, New York, 930 pp.
- Karavalakis, G., Jiang, Y., Yang, J., Durbin, T., Nuottimäki, J. & Lehto, K. 2016. Emissions and Fuel Economy Evaluation from Two Current Technology Heavy-Duty Trucks Operated on HVO and FAME Blends. *SAE International Journal of Fuels and Lubricants* **9**(1), 15 p.
- Murphy, J.M. 1983. An Improved Cetane Number Predictor for Alternative Fuels. *SAE Technical paper* **831746**, 12 p.
- Napolitano, P., Beatrice, C., Guido, C., Del Giacomo, N., Pellegrini, L. & Scorletti, P. 2015. Hydrocracked Fossil Oil and Hydrotreated Vegetable Oil (HVO) Effects on Combustion and Emissions Performance of ‘Torque-Controlled’ Diesel Engines. *SAE International Journal of Fuels and Lubricants* **9**(1), 14 p.

- Neste Group. 2016. *Neste Renewable Diesel Handbook*. Neste, Espoo, 57 pp.
- Pellegrini, L., Beatrice, C. & Di Blasio, G. 2015. Investigation of the Effect of Compression Ratio on the Combustion Behavior and Emission Performance of HVO Blended Diesel Fuels in a Single-Cylinder Light-Duty Diesel Engine. SAE Technical Paper 2015-01-0898, 17 p.
- Pexa, M., Čedík, J., Mařík, J., Hönig, V., Horníčková, Š & Kubín, K. 2015. Comparison of the operating characteristics of the internal combustion engine using rapeseed oil methyl ester and hydrogenated oil. *Agronomy Research* **13**(2), 613–620.
- Sajjad, H., Masjuki, H.H., Varman, M., Kalam, M.A., Arbab, M.I., Imtenan, S. & Rahman, S.M. 2014. Engine combustion, performance and emission characteristics of gas to liquid (GTL) fuels and its blends with diesel and bio-diesel. *Renewable and Sustainable Energy Reviews* **30**, 961–986.
- Sondors, K., Birkavs, A., Dukulis, I., Pirs, V. & Jesko, Z. 2014. Investigation in tractor Claas Ares 557ATX operating parameters using hydrotreated vegetable oil fuel. In: *Engineering for Rural Development* **13**, LUA, Jelgava, pp. 63–68.
- Sugiyama, K., Goto, I., Kitano, K., Mogi, K. & Honkanen, M. 2011. Effects of Hydrotreated Vegetable Oil (HVO) as Renewable Diesel Fuel on Combustion and Exhaust Emissions in Diesel Engine. *SAE International Journal of Fuels and Lubricants* **5**(1), 13 p.
- Stone, R. 1999. *Introduction to Internal Combustion Engines*. Third Edition. Palgrave Macmillian, New York. 641 pp.